Redox Chemistry and Acid−Base Equilibria of Mitochondrial Plant Cytochromes *c*†

Gianantonio Battistuzzi,‡ Marco Borsari,‡ James A. Cowan,§ Christoph Eicken,|| Lodovica Loschi,‡ and Marco Sola*,‡

Department of Chemistry, University of Modena and Reggio Emilia, Via Campi 183, 41100 Modena, Italy, Department of Chemistry, The Ohio State University, 120 West 18th Avenue, Columbus, Ohio 43210, and Anorganisch-Chemisches Institut der Universität Münster, Wilhelm-Klemm Strasse, 848149 Münster, Germany

Received October 13, 1998; Revised Manuscript Received February 2, 1999

ABSTRACT: Mitochondrial cytochromes *c* from spinach, cucumber, and sweet potato have been investigated through direct electrochemical measurements and electronic and ^{1}H NMR spectroscopies, under conditions of varying temperature and pH. The solution behaviors of these plant cytochromes closely resemble, but do not fully reproduce, those of homologous eukaryotic species. The reduction potentials ($E^{\circ\prime}$) at pH 7 and 25 °C are +0.268 V (spinach), +0.271 V (cucumber), and +0.274 V (sweet potato) vs SHE. Three acid−base equilibria have been determined for the oxidized proteins with apparent pK_a values of 2.5, 4.8, and 8.3−8.9, which are related to disruption of axial heme ligation, deprotonation of the solvent-exposed heme propionate-7 and replacement of the methionine axially bound to the heme iron with a stronger ligand, respectively. The most significant peculiarities with respect to the mammalian analogues include: (i) less negative reduction enthalpies and entropies ($\Delta S^{\circ\prime}_{rc}$ and $\Delta H^{\circ\prime}_{rc}$) for the various protein conformers [low- and high-T native (N_1 and N_2) and alkaline (A)], whose effects at pH 7 and 25 °C largely compensate to produce $E^{\circ\prime}$ values very similar to those of the mammalian proteins; (ii) the $N_1 \rightarrow N_2$ transition that occurs at a lower temperature (e.g., 30−35 °C vs 50 °C at pH 7.5) and at a lower pH (7 vs 7.5); and (iii) a more pronounced temperature-induced decrease in the pK_a for the alkaline transition which allows observation of the alkaline conformer(s) at pH values as low as 7 upon increasing the temperature above 40 °C. Regarding the pH and the temperature ranges of existence of the various protein conformers, these plant cytochromes *c* are closer to bacterial cytochromes c_2.

Class-I *c*-type cytochromes (cyt)[1] are a large family of structurally homologous heme proteins which shuttle electrons between the membrane-bound protein complexes involved in the energy-producing electron-transport chains of bacterial photosynthesis and mitochondrial respiration. These globular proteins have been thoroughly investigated in terms of three-dimensional structure, electronic properties of the heme, redox potentials, and the mechanism and kinetics of electron exchange (*1*−*3*). Among eukaryotic cytochromes *c*, those from plant mitochondria have received significantly less attention in the past as compared to their mammalian and yeast analogues. The three-dimensional structure of the species from rice, the only structure of a plant cytochrome *c* solved to date (*4*), shows that the main chain conformation is almost identical to that of the animal proteins, except for the presence of eight additional residues at the N-terminus, which is acetylated. This terminal polypeptide segment is located on the opposite side of the putative binding site of the protein with its redox partner (cytochrome *c* oxidase or reductase) and adopts a relatively extended conformation that is stabilized by a hydrogen bond network connecting four of its residues with the remainder of the protein. The fact that several amino acids involved in this interaction are conserved in all plant cytochromes *c* known to date strongly suggests that the conformation of the N-terminal extension is maintained in all these proteins. Moreover, two of the lysine residues involved in the binding site for the electron exchange with the redox partner, namely, Lys72 and Lys86, are trimethylated. As noted elsewhere, the close structural similarity between plant and animal cytochromes *c* should in principle result in rather conserved physicochemical and biological properties for these two protein families (*4*). However, various aspects of the solution chemistry of the plant species, such as acid−base equilibria, pH- and temperature-induced conformational changes, and redox properties, are still largely uncharacterized, and constitute the goal of this work. Here, we report on the electronic and ^{1}H NMR spectral properties, and the redox behavior of cytochromes *c* from spinach (*Spinacea oleracea*), cucumber (*Cucumis sativus*), and sweet potato (*Ipomoea batatas*) studied as a function of pH and temperature. This approach has allowed determination of the acid−base equilibria affecting the redox behavior and the coordination and electronic properties of the heme, and of the thermodynamics of the electron exchange. These data indicate that

† This work was supported by the Ministero della Ricerca Scientifica e Tecnologica of Italy (Progetti di Rilevante Interesse Nazionale) and the Consiglio Nazionale delle Ricerche, Comitato Scienze Chimiche (Progetto Bilaterale) of Italy.

* To whom correspondence should be addressed.

‡ Department of Chemistry, University of Modena and Reggio Emilia.

§ Department of Chemistry, The Ohio State University.

|| Anorganisch-Chemisches Institut der Universität Münster.

[1] Abbreviations: cyt, cytochrome; SCE, saturated calomel electrode; SHE, standard hydrogen electrode; N, native cytochrome *c*; N_1, low-temperature conformer of native cytochrome *c*; N_2, high-temperature conformer of native cytochrome *c*; A, alkaline conformer of cytochrome *c*.

10.1021/bi982429x CCC: $18.00
Published on Web 04/09/1999

the plant species are related to other eukaryotic (mammalian) class-I cytochromes *c* on thermodynamic grounds, but exhibit some peculiar properties regarding the pH and the temperature ranges in which the various protein conformers exist, and do in fact show more extensive analogies with the bacterial c_2 species.

EXPERIMENTAL PROCEDURES

Protein Purification. All purification steps were carried out aerobically at 4 °C, unless otherwise specified; 6 kg of fresh spinach and 40 kg of cucumbers were washed, and the leaves (4 kg, removed from the stems) and the peelings (3 kg), respectively, were passed through a domestic juicer, obtaining approximately 2 L of a dark green suspension. The residual solid material was suspended in 3 L of 10 mM phosphate buffer at pH 6 and homogenized with a Wharing Blender. The dark green homogenate was filtered through a cheesecloth to remove debris, added to the suspension obtained from juicing, and then centrifuged for 30 min at 5000 rpm in an ALC-3245A centrifuge. The light green supernatant was brought to 40% saturation of $(NH_4)_2SO_4$ (240 g/L), stirred for 3 h, and then centrifuged for 45 min at 8000 rpm to remove the precipitate. Solid $(NH_4)_2SO_4$ was added to the light brown supernatant up to full saturation (300 g/L). The suspension was stirred overnight, and the precipitate, collected after 2 h of centrifugation at 8000 rpm, was dissolved in 250 mL of 50 mM Tris-HCl, pH 7.3, and stirred for 24 h. The undissolved material was removed by centrifugation, and the brown supernatant was dialyzed against several changes of 20 mM Tris-HCl, pH 7.3, to decrease ionic strength, and then applied to a DEAE-cellulose (Whatman DE-52) column (7 × 12 cm) equilibrated with the same buffer. The fractions not retained by the column, containing the basic proteins, were collected and concentrated in an ultrafiltration Amicon flow cell (YM-5 membrane). The reddish solution was dialyzed against three changes of 20 mM phosphate buffer, pH 5.5, and then loaded onto a SP−Sepharose HP (Pharmacia) column (2.6 × 15 cm) equilibrated with the same buffer. The column was washed with 3 volumes of the loading buffer and then eluted with a linear gradient from 0 to 0.3 M NaCl in 20 mM phosphate buffer, pH 5.5. The cytochrome *c* was eluted at 0.18−0.23 M NaCl. After concentration, solid $(NH_4)_2SO_4$ was added to a final concentration of 2 M. The resulting solution was applied to a Phenyl Sepharose FF (Pharmacia) column (1.5 × 10 cm) preequilibrated with 3 volumes of 1.8 M $(NH_4)_2SO_4$ in 50 mM phosphate buffer, pH 7.0. The column was washed with 1 volume of loading buffer and then with a linear gradient from 1.8 to 0 M $(NH_4)_2SO_4$ in 50 mM phosphate buffer, pH 7.0. The cytochrome *c* was eluted at 1.2−1.1 M $(NH_4)_2SO_4$. The fractions containing the cytochrome *c* were concentrated, and then loaded on a HiLoad 16/60 Superdex 75 prep grade column (Pharmacia) and eluted with 0.15 M NaCl in 10 mM phosphate buffer, pH 7.0. An analogous procedure was followed for the purification of sweet potato cytochrome *c*: the only variants were a gel filtration step on a Sephacryl S-200 column after precipitation with $(NH_4)_2SO_4$, and a final chromatography on hydroxyapatite.

Molecular Weight Determination. The molecular weight of the proteins was determined by SDS−polyacrylamide gel electrophoresis using a Mini-PROTEAN II system (Bio Rad). The molecular weight markers used for electrophoresis were myosin (200 000), β-galactosidase (116 000), phosphorylase B (97 400), bovine serum albumin (67 000), ovalbumin (43 000), carbonic anhydrase (31 000), trypsin inhibitor (21 500), lysozyme (14 500), and aprotinin (6500).

Electrochemical Measurements. Cyclic voltammetry experiments were carried out with a Potentiostat/Galvanostat PAR Model 273A at different scan rates (from 0.02 to 1 V s^{-1}) using a cell for small volume samples (0.5 mL) under argon. A 2 mm diameter gold disk was used as working electrode, with a Pt sheet and a saturated calomel electrode (SCE) as counter and reference electrode, respectively. The electric contact between the SCE and the working solution was obtained with a Vycor set. Potentials were calibrated against the MV^{2+}/MV^{+} couple (MV = methyl viologen) (*5*). All the redox potentials reported here are referred to the standard hydrogen electrode (SHE). The working electrode was cleaned by first dipping it in ethanol for 10 min, and then polishing it with an alumina (BDH, particle size of about 0.015 mm) water slurry on cotton wool; finally the electrode was treated in an ultrasonic pool for about 10 min. To minimize residual adsorbed impurities, the electrode was first set at +1 V (vs SCE) for 180 s, and then subjected to 10 voltammetric cycles between +0.7 and −0.6 V at 0.1 V s^{-1}. Modification of the electrode surface was performed by dipping the polished electrode into a 1 mM solution of 4-mercaptopyridine for 30 s, and then rinsing it with Nanopure water; 0.1 M NaCl was used as base electrolyte. The experiments were performed several times, and the reduction potentials were reproducible within ±2 mV. Protein solutions, made in 10 mM phosphate buffer, 0.1 M NaCl, were freshly prepared before use, and their concentration, varying over 0.1−0.3 mM, was checked spectrophotometrically. The pH was changed by adding small amounts of concentrated NaOH or HCl under fast stirring. Variable-temperature experiments were performed with a nonisothermal electrochemical cell (*6*, *7*). The reference electrode (SCE) was kept at constant temperature (21 ± 0.1 °C), while the half-cell containing the working electrode and the Vycor junction to the reference electrode were kept under thermostatic control with a water bath, and its temperature varied from 4 to 60 °C. With this experimental configuration, the reaction entropy ($\Delta S^{\circ\prime}_{rc}$) for reduction of ferricytochrome *c* is given by (*6*−*8*)

$$\Delta S^{\circ\prime}_{rc} = S^{\circ\prime}_{red} - S^{\circ\prime}_{ox} = nF(dE^{\circ\prime}/dT)$$

Thus, $\Delta S^{\circ\prime}_{rc}$ was determined from the slope of the plot of $E^{\circ\prime}$ versus temperature. The enthalpy change ($\Delta H^{\circ\prime}_{rc}$) was obtained from the Gibbs−Helmholtz equation, namely, from the slope of the $E^{\circ\prime}/T$ versus $1/T$ plot. The nonisothermal behavior of the cell was carefully checked by determining the $\Delta H^{\circ\prime}_{rc}$ and $\Delta S^{\circ\prime}_{rc}$ values of the ferricyanide/ferrocyanide couple (*6*−*9*).

Spectroscopic Measurements. Electronic spectra were recorded on a Perkin-Elmer Lambda 19 spectrophotometer at 25 ± 0.1 °C. ^{1}H NMR spectra were run on a Bruker AMX-400 spectrometer at 400.13 MHz. Typical acquisition parameters were as follows: pulse width, 6.8 ms (90° pulse); pulse delay, 0.5 s; number of scans, 512−2048. Spectra were run on 0.1−0.3 mM protein samples in aqueous solutions containing 10% deuterium oxide (D_2O) and were referenced

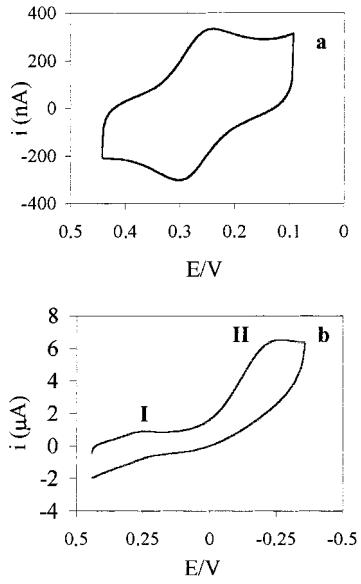

FIGURE 1: Cyclic voltammograms of cucumber cytochrome *c* at a 4-mercaptopyridine surface-modified gold disk electrode. (a) pH 7, $T = 298$ K; (b) pH 9.5, $T = 308$ K (I and II refer to the waves of the native and alkaline conformer, respectively). Sweep rate, 50 mV s^{-1}. Protein concentration, 0.1 and 0.3 mM in (a) and (b), respectively. Base electrolyte, 0.1 M NaCl in 10 mM phosphate buffer. Almost identical electrochemical responses were obtained from the species from sweet potato and spinach.

to tetramethylsilane (TMS) after calibration against the HDO peak, set at 4.78 ppm from TMS at 20 °C. Water peak suppression was achieved using the super-WEFT pulse sequence (*10*). Calibration of the temperature control unit of the spectrometer was achieved by recording the spectra of ethylene glycol in water−dimethyl sulfoxide at different temperatures.

RESULTS

Proteins. Approximately 4, 3, and 3 mg of pure cytochrome *c* were obtained from 4 kg of fresh spinach leaves, 40 kg of cucumbers, and 50 kg of sweet potatoes, respectively. All cytochromes gave a single band at about 12 000 Da on SDS−PAGE electrophoresis, in agreement with the molecular mass expected from the amino acid sequence of spinach (*11*) and sweet potato (*12*) cytochrome *c*. The purity index ($\epsilon_{550,reduced}/\epsilon_{280,oxidized}$) was 1.0, 1.1, and 1.1 for spinach, sweet potato, and cucumber cyt *c*, respectively.

Cyclic Voltammetry. A typical cyclic voltammogram of these plant cytochromes *c*, obtained with a 4-mercaptopyridine surface-modified Au electrode at pH 7, is shown in Figure 1a. In these conditions, all proteins demonstrated well-behaved electrochemistry. The electrochemical processes were reversible and diffusion-controlled, as indicated by peak separations of 59 ± 2 mV for scan rates in the range 10−500 mV s^{-1}, and by the anodic and cathodic peak currents which were identical and also proportional to both the protein concentration and $v^{1/2}$ (v = scan rate). For all cytochromes, estimation of the total charge needed for full reduction of the oxidized form subject to cathodic electrolysis at −0.1 V (versus SCE) (*13*) showed that a one-electron reduction process had occurred. Taken together, these data unequivocally show that the electron transfer between the cytochromes and the Au electrode is fast and does not involve protein adsorption and/or denaturation onto the electrode surface. Thus, we are measuring the electrochemistry of the Fe^{3+}/Fe^{2+} equilibrium of the heme iron of bulk cytochromes, and the $E^{\circ\prime}$ can be taken as the average of the cathodic and anodic peak potentials. $E^{\circ\prime}$ values of +0.268, +0.271, and +0.274 V (vs SHE) at pH 7.0 were obtained for spinach, cucumber, and sweet potato cytochromes *c*, respectively (Table 1).

Table 1: Reduction Potentials ($E^{\circ\prime}$) at 25 °C for the Native (N) and Alkaline (A) Forms of Plant Cytochromes *c*, and $\Delta H^{\circ\prime}_{rc}$ (kJ mol^{-1}) and $\Delta S^{\circ\prime}_{rc}$ (J mol^{-1} K^{-1}) Values Determined from the Temperature Dependence of the Reduction Potential[a]

				$\Delta S^{\circ\prime}_{rc}$		$\Delta H^{\circ\prime}_{rc}$	
cyt *c*	pH	$E^{\circ\prime}_N$	$E^{\circ\prime}_A$	native	alkaline	native	alkaline
spinach	7.0	+0.268		−29		−35	
				−58		−43	
	7.5	+0.268	−0.112	−27	−33	−34	+1
				−58		−43	
	8.4	+0.267	−0.121	−20	−40	−32	0
				−58		−43	
cucumber	7.0	+0.271		−23		−33	
				−58		−44	
	7.5	+0.270	−0.164	−19	−38	−32	+4
				−64		−46	
	8.5	+0.268	−0.173	−13	−41	−30	+4
				−64		−46	
sweet potato	7.0	+0.274		−31		−36	
				−77		−50	
	7.6	+0.274	−0.145	−24	−41	−34	+2
				−79		−51	
	8.4	+0.272	−0.153	−17	−47	−31	+1
				−106		−59	

[a] The native and alkaline forms correspond to waves I and II in the cyclic voltammograms, respectively (see Figure 1). Measurements were performed in 10 mM phosphate buffer, 0.1 M NaCl. Values in the upper and lower rows for the native species refer to the low-T (N_1) and high-T (N_2) conformer, respectively. Errors on $\Delta H^{\circ\prime}_{rc}$ and $\Delta S^{\circ\prime}_{rc}$ values are ±2 (kJ mol^{-1}) and ±6 (J mol^{-1} K^{-1}), respectively (expressed as the upper values of the standard deviations for the data points).

Electronic and ^{1}H NMR Spectra. The electronic spectra of the reduced cytochromes *c* are nearly identical to those of other eukaryotic species. For all species, the Soret band falls at 415 nm and the α and β bands at 550 and 520 nm, respectively. In the oxidized form, the Soret band moves to 408 nm, the α and β bands collapse to one large band at 530 nm with a shoulder at 560 nm, and the typical band associated with the methionine sulfur→Fe charge-transfer transition appears at 695 nm (not shown). The hyperfine-shifted resonances in the 400 MHz ^{1}H NMR spectrum of the proteins as isolated in aerobic conditions at pH 7 are shown in Figure 2. The signal patterns are very similar and closely resemble those of the horse heart and yeast proteins, which have been fully assigned (*14*−*18*). Preliminary data obtained through two-dimensional NOESY and COSY experiments (*12*) show that the three proton peaks *a*, *b*, and *m* correspond to the heme methyl groups in positions 8, 3, and 5 [thus indicating that the order of decreasing frequency for the heme methyl groups in mitochondrial cytochromes *c* and bacterial cytochromes c_2, namely, 8, 3, 5, 1 (*14*−*21*), is conserved also in the plant species], peak *c* to the $CH\epsilon_1$ of the iron binding His18, and peak *d* to one Hα proton of the heme propionate-7. Moreover, the region between 10 and 15 ppm (peaks *e*−*l*) contains, among others, one CHβ proton of His18 and the second Hα proton of the heme propionate-

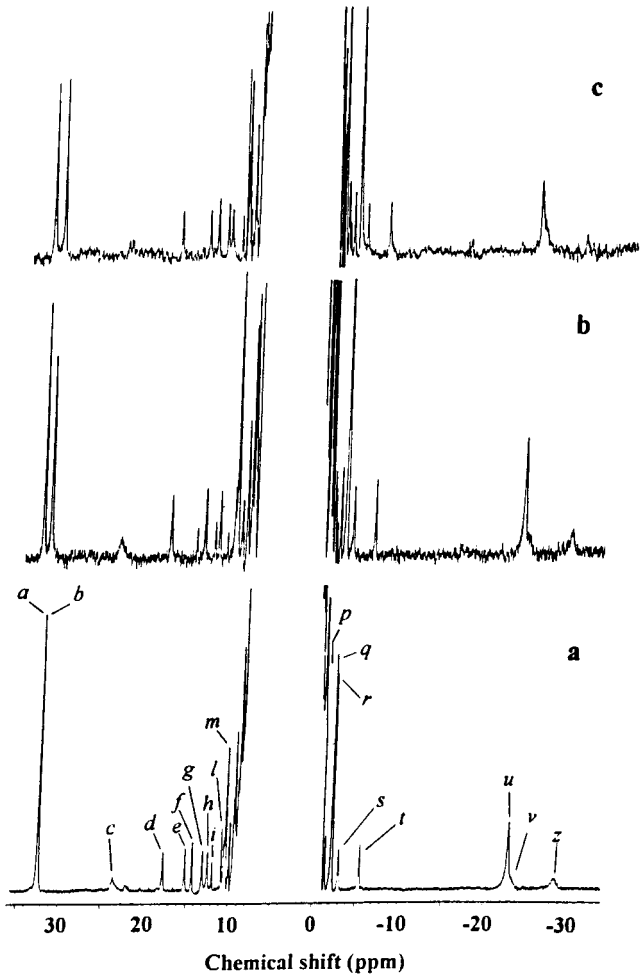

FIGURE 2: 400 MHz ^{1}H NMR spectra of ferricytochromes *c* from (a) spinach, (b) sweet potato, and (c) cucumber. Spectra were recorded in water at 300 K. Protein concentration was 0.5 mM in 0.1 M NaCl, 10 mM phosphate buffer at pH 7.

7. The low-frequency paramagnetic resonances *u*, *v*, and *z* correspond to the ϵ-methyl group of the iron binding Met80, to the CHδ proton of His18, and to a γ-methylene proton of the methionine ligand, respectively. The complete assignment of the paramagnetic resonances to individual heme substituents and nearby residues is currently underway in our laboratory. The small, though measurable, differences in chemical shift of the signals of the heme substituents between plant and mitochondrial cytochromes *c* are likely the result of a slightly different unpaired electron spin distributions on the heme, most probably due to small differences in the orientation of the axial ligands (*14*). It is worthy of note that the spectrum of spinach cyt *c* is the first case reported to date in which the 8-CH_3 and 3-CH_3 heme methyl resonances have the same chemical shift at pH 7.

Effects of pH on the Electrochemical Properties and Spectral Features. In the pH range 7.5−5.5, all cytochromes yield a well-behaved voltammetric signal (wave I), due to the Fe^{3+}/Fe^{2+} equilibrium of the heme iron (Figure 1a). Peak currents and $E^{\circ\prime}$ values remain nearly constant, indicating that in this pH range no acid/base equilibria influence their redox properties. At pH values below 5.5, the electrochemical response is less well-defined: the separation between the anodic and cathodic peaks increases, and they become broader. This is accompanied by a decrease in current intensity, particularly that of the anodic peak which disappears below pH 4. This means that below pH 5.5 the electrochemical reversibility is progressively lost. Moreover, even using high scan rates, the peak currents do not linearly depend on $v^{1/2}$; i.e., the process is no longer diffusion-controlled. These effects are most likely due to the protonation of the pyridine nitrogen of the promoter (*22*−*24*), that makes the interaction with the positively charged protein unfavorable on electrostatic grounds. At pH values above 7.5, a new diffusion-controlled chemically irreversible signal (wave II) appears at negative potentials (E_{pc} = −0.152, −0.196, and −0.176 V vs SHE for spinach, cucumber, and sweet potato cyt *c*, respectively) (Figure 1b), which is due to the alkaline conformer (state IV) of cytochrome *c* (*1*, *2*, *25*, *26*) (A form thereafter). The intensity of the anodic counterpart increases with increasing scan rate, and becomes comparable to that of the cathodic peak using scan rates higher than 0.6 V s^{-1}. For all the species, the electrochemical behavior of wave II improves with increasing temperature, as observed elsewhere for other class I cytochromes *c* (*25*). However, the observation of the return anodic peak at relatively low sweep rates and the decrease of peak separation in the cyclic voltammograms occur at lower temperatures in comparison to the mammalian species (*25*) (for example, peak separations at pH 8.5 were of approximately 0.07 V at 40 °C, against 55 °C for the mammalian analogues, using a sweep rate of 0.4 V s^{-1}). We note that in this respect the behavior of these plant cytochromes *c* is closer to that of bacterial cytochromes c_2 (*25*). Upon increasing the pH in the range 7.5−9.5, the cathodic peak current of wave II invariably increases to the detriment of wave I (Figure 3), while their sum remains constant and linearly dependent on $v^{1/2}$. Current intensities titrate with a pK_a value of 8.9 ± 0.1, 8.4 ± 0.1, and 8.4 ± 0.1 for the species from spinach, cucumber, and sweet potato, respectively. In the pH range 7.5−10, the anodic and cathodic peak potentials of both waves remain roughly constant. Upon raising the pH above 10.5, the formation of a precipitate is observed due to partial protein denaturation.

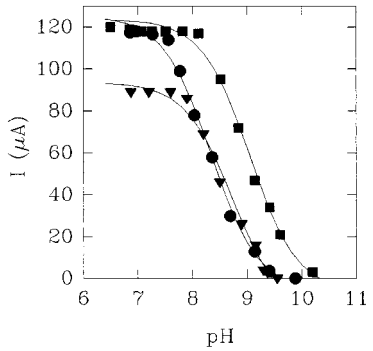

FIGURE 3: pH dependence of the cathodic peak current intensity of wave I for cytochrome *c* from spinach (■), cucumber (●), and sweet potato (▼). Solid lines are fits to the conventional one-proton equilibrium equation:

$$I_{obs} = (I_{cyt}K_a + I_{cytH}[H^+])/(K_a + [H^+])$$

(where I_{obs} is the observed peak intensity; I_{cyt} and I_{cytH} those of the high-pH and low-pH form, respectively). Measurements were carried out in 0.1 M NaCl, 10 mM phosphate. T = 298 K.

The electronic spectra of the cytochromes as isolated at neutral pH clearly indicate that the proteins are fully oxidized. No spectral changes are detected in the pH range 4−8, as found for other class I cytochromes *c* (*2*, *27*, *28*). Upon

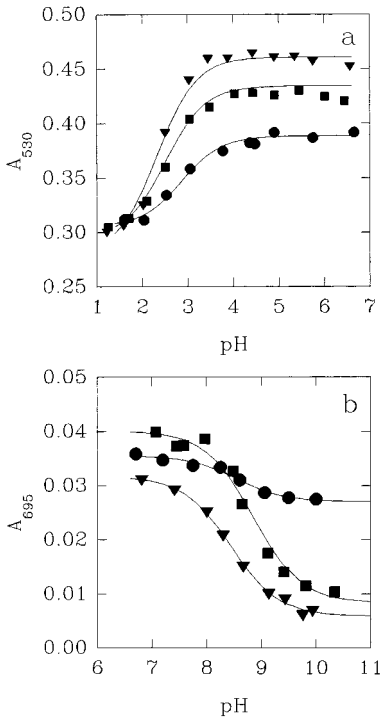

FIGURE 4: Intensities of the electronic bands at (a) 530 nm and (b) 695 nm as a function of pH for the species from spinach (■), cucumber (●), and sweet potato (▼). Measurements were carried out in 0.1 M NaCl, 10 mM phosphate. $T = 298$ K. Solid lines are fits to a one-proton equilibrium equation.

lowering the pH below 4, the bands of the native form decrease in intensity, and a new band appears at 625 nm, which is typical of high-spin heme Fe(III) (not shown). The absorbances at 530 and 625 nm could be fit to a one-proton equilibrium equation obtaining apparent pK_a values of 2.5 ± 0.1 (spinach), 2.6 ± 0.1 (cucumber), and 2.4 ± 0.1 (sweet potato) (Figure 4a). Moreover, in the pH range 7−11, the intensity of the 695 nm band of the ferricytochromes decreases with increasing pH with an apparent pK_a of 8.8 ± 0.1 (spinach), 8.6 ± 0.1 (cucumber), and 8.4 ± 0.1 (sweet potato) (Figure 4b). The latter equilibrium is due to disruption of the axial Fe−S(Met) axial bond in the alkaline conformer of the cytochromes.

The ^{1}H NMR spectra of oxidized spinach cyt *c* are shown in Figure 5 for selected pH values in the range 5−11. The other species show identical pH-dependent spectral properties. In the pH range 4−6, the chemical shifts of many hyperfine-shifted ^{1}H NMR signals show pH titration profiles that can be fit with a one-proton equilibrium equation, yielding pK_a values of 4.8 ± 0.1, 4.7 ± 0.1, and 4.7 ± 0.1 for spinach, cucumber, and sweet potato cytochromes *c*, respectively. Figure 6a shows the pH profile for the chemical shift of one Hα proton of the heme propionate-7 (peak *d* in Figure 2). The chemical shift and the line width of the hyperfine-shifted ^{1}H NMR resonances remain almost unchanged for all cytochromes in the pH range 5−11, while the signal intensities are remarkably pH-dependent. In particular, at pH values above 7.5, a new group of signals appears between 10 and 25 ppm in slow exchange on the NMR time scale (Figure 5). The intensity of these resonances increases with pH to the detriment of the intensity of the peaks of the neutral form, which titrates with a pK_a value of 8.7 ± 0.1, 8.3 ± 0.1, and 8.2 ± 0.1 for the proteins from

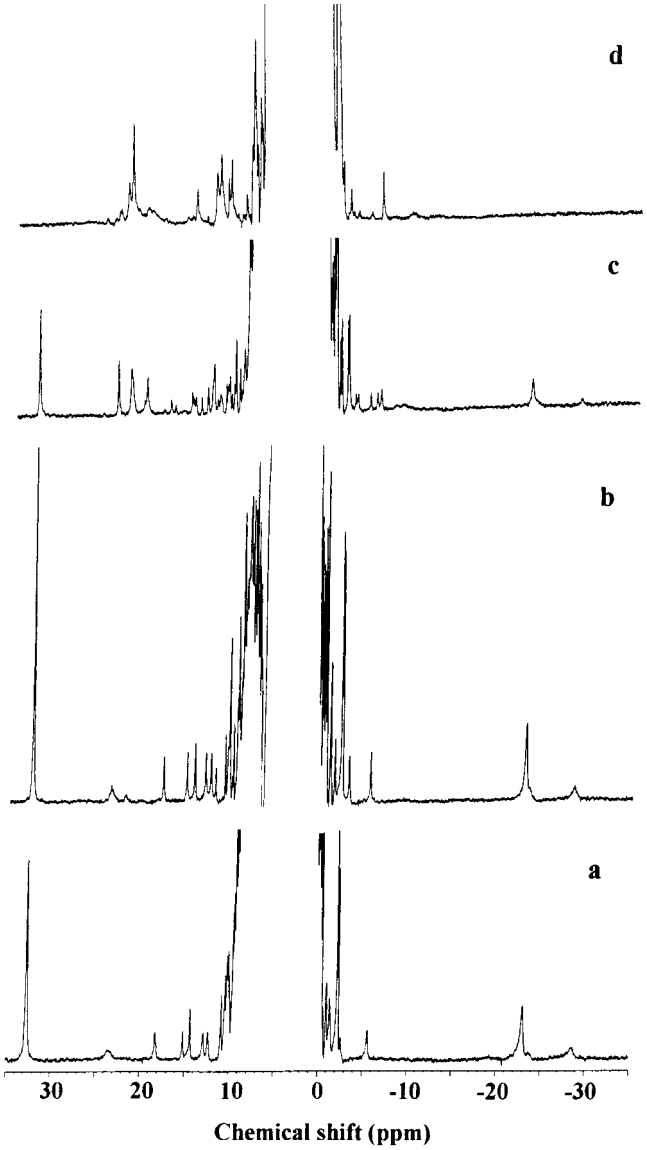

FIGURE 5: 400 MHz ^{1}H NMR spectra of spinach ferricytochrome *c* at different pH values. (a) pH 5.0; (b) pH 7.2; (c) pH 9.1; (d) pH 10.6. Spectra were recorded in water at 298 K. Protein concentration was 1 mM in 0.1 M NaCl, 10 mM phosphate.

spinach, cucumber, and sweet potato, respectively (Figure 6b). This new signal pattern, still indicative of a low-spin ferriheme, corresponds to the alkaline conformer of the cytochromes. The A form is known to differ from the native forms in axial heme iron ligation, most likely due to substitution of a lysine for the methionine ligand (*2*, *29*−*52*). A close inspection of the pH-induced intensity changes of the new peaks suggests the existence of at least two alkaline isomers, one of which prevails on the other at high pH. This behavior parallels that of several eukaryotic and bacterial class I cytochromes *c* (*25*, *40*, *41*). Below pH 4 all the hyperfine-shifted resonances invariably decrease in intensity upon decreasing pH, and the integrated area of the methyl peaks titrates with an apparent pK_a value of 2.5 for all species. This is paralleled by the appearance of a new set of broader and more shifted peaks in slow exchange on the NMR time scale, which is typical of a high-spin Fe(III) heme (*14*) (not shown). Upon returning the pH to 7, the spectrum of the low-spin Fe(III) heme of the neutral form is fully restored.

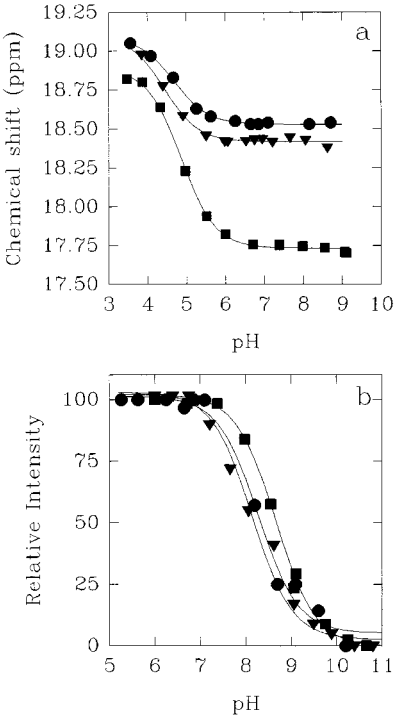

FIGURE 6: pH dependence of (a) the chemical shift of the ^{1}H NMR resonance of one Hα proton of the heme propionate-7 and (b) the intensity (from the integrated area) of the ^{1}H NMR resonance of the heme 8-CH_3 group for the cytochromes *c* from spinach (■), cucumber (●), and sweet potato (▼). (The intensities of the other heme methyl groups and of the ε-CH_3 of the iron binding methionine show identical pH dependencies.) Solid lines are fits to a one-proton equilibrium equation. $T = 298$ K.

Effects of Temperature on the Redox and Spectral Properties. Thermodynamic Parameters of the Redox Process. The temperature dependence of the reduction potential of the three cytochromes at different pH values is illustrated in Figure 7. At pH 7, the reduction potential of the native form (wave I) linearly decreases with increasing temperature from 4 to 55 °C (Figure 7a). The plot is clearly biphasic with a transition point at 33, 40, and 40 °C for spinach, cucumber, and sweet potato cytochrome *c*, respectively. The temperature of the break decreases with increasing pH (Figure 7b,c). This behavior was already described in detail for horse and beef heart cytochromes *c* and bacterial cytochromes c_2 (*22*, *25*, *53*−*55*) and assigned to a conformational change of the native ferri-form (*55*), which may thus exist in a low-*T* and high-*T* conformation (called N_1 and N_2, respectively). The reduction potential of the alkaline form (wave II) linearly decreases with increasing temperature (Figure 7b,c); in parallel, the currents of both anodic and cathodic peaks of wave II increase to the detriment of those of the native form (wave I), due to the T-induced depression of the pK_a for the alkaline transition (*33*).

The thermodynamic parameters determined from the nonisothermal experiments described above are reported in Table 1. Reduction entropies are invariably negative for the neutral and alkaline conformers of all species. Reduction enthalpies are negative for the neutral forms and slightly positive for the alkaline species. The $\Delta S^{\circ\prime}_{rc}$ and $\Delta H^{\circ\prime}_{rc}$ values for the various conformers are of the same order of magnitude of those determined previously for other mitochondrial and bacterial class I cytochromes *c* in the same conditions (*25*).

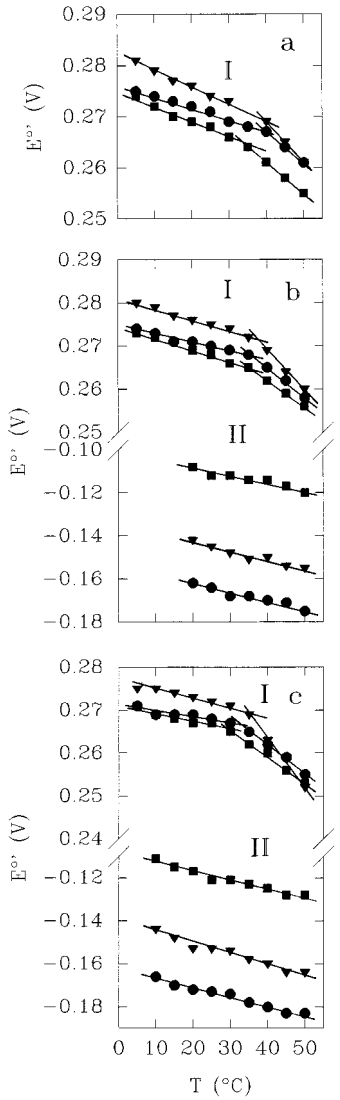

FIGURE 7: Temperature dependence of the reduction potential of cytochromes *c* from spinach (■), cucumber (●), and sweet potato (▼) at (a) pH 7.0, (b) pH 7.5, and (c) pH 8.5. Base electrolyte, 0.1 M NaCl in 10 mM phosphate buffer. Solid lines are least-squares fits to the data points. I and II refer to the reduction potentials of wave I (native cyt *c*) and wave II (alkaline cyt *c*), respectively.

Proton NMR spectra were run from 15 to 60 °C at pH 7, focusing on the changes in the hyperfine-shifted resonances (Figure 8). The T-induced spectral changes for these plant cytochromes are closely similar. In particular, (i) the chemical shift of most of the heme methyl peaks decreases linearly with increasing temperature following a Curie law temperature behavior: the linear Curie plot of the heme methyl groups shows a slight discontinuity at a temperature of approximately 36, 40, and 40 °C for spinach, cucumber, and sweet potato cyt *c*, respectively (Figure 9), which is almost coincident with that of the break in the $E^{\circ\prime}/T$ profile of wave I (Figure 7a): this behavior reproduces that of other class 1 cyt *c* (*25*, *56*); (ii) a new set of hyperfine-shifted signals similar to that of the alkaline form at room temperature appears in the ^{1}H NMR spectra of spinach, cucumber, and sweet potato cyt *c* at 37, 42, and 42 °C, respectively (Figure 8), and its intensity increases with increasing temperature to the detriment of that of the native form. As previously reported for other cytochromes *c* (*25*, *29*, *33*), the spectral features of these hyperfine-shifted resonances show that there

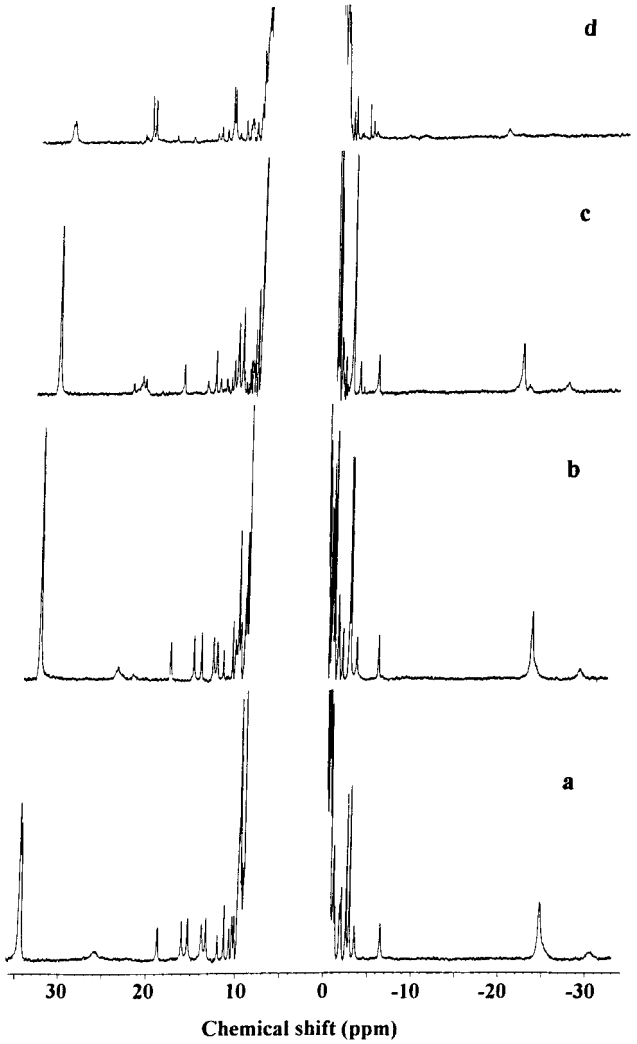

FIGURE 8: 400 MHz ^{1}H NMR spectra of spinach cytochrome *c* at different temperatures. (a) 285 K; (b) 300 K; (c) 315 K; (d) 330 K. Spectra were recorded in water at pH 7. Protein concentration was 0.3 mM in 0.1 M NaCl, 10 mM phosphate buffer.

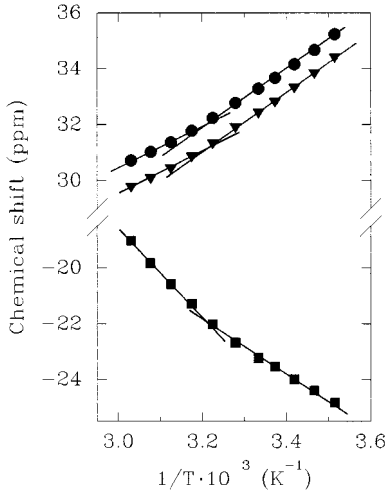

FIGURE 9: Curie plot for some ^{1}H NMR heme methyl peaks of sweet potato cyt *c* at pH 7. 8-CH_3 (●); 5-CH_3 (▼); (■) ϵ-CH_3 of the iron binding Met80. Analogous plots were obtained for the other plant cyt *c*.

exist at least two high-*T* conformers with different molar ratios (from approximately 1:10 for spinach cyt *c* to 1:1 for cucumber and sweet potato cyt *c*).

DISCUSSION

Proteins. Spinach and rice cyt *c* show an 84% sequence identity (*2*). This allows the three-dimensional structure of the latter species to be used to interpret, at least to a first approximation, the physicochemical properties of the former. Sweet potato cyt *c* shows a sequence identity close to 90% with spinach cyt *c* (*12*). No information is presently available for cucumber cyt *c*, but its nearly identical molecular weight and overall charge with spinach cyt *c* suggests that the two species should be closely sequence-related.

Redox Properties and Thermodynamics of Electron Exchange. Protein reduction in cytochromes *c* is accompanied by negative enthalpy and entropy changes (*25*, *56*, *57*). The first term is mainly the result of stabilization of the Fe^{2+} state due to ligand binding interactions, the hydrophobic environment at the heme−protein interface, and the limited accessibility of the heme to the solvent. The entropy loss is instead likely related to a greater conformational flexibility of the oxidized as compared to the reduced form (*15*, *16*, *25*, *58*) and to differences in solvation properties between the two redox states (*56*, *59*, *60*).

The $\Delta S^{\circ\prime}_{rc}$ and $\Delta H^{\circ\prime}_{rc}$ values for the low-*T* conformer (N_1) of the neutral form of plant cytochromes *c* are rather similar (Table 1) and are both less negative than those for the mammalian analogues in the same conditions (*22*, *25*, *55*, *57*). The average enthalpic and entropic contributions to $E^{\circ\prime}$ at pH 7 and 25 °C are $-\Delta H^{\circ\prime}_{rc}/F = +0.359$ V and $T\Delta S^{\circ\prime}_{rc}/F = -0.086$ V for the plant species vs $-\Delta H^{\circ\prime}_{rc}/F = +0.430$ V and $T\Delta S^{\circ\prime}_{rc}/F = -0.170$ V for the mammalian species (*25*). Thus, the $E^{\circ\prime}$ values in these conditions for spinach, cucumber, and sweet potato cyt *c* ($E^{\circ\prime} = +0.268$, $+0.271$, and $+0.274$ V, respectively) turn out to be very similar to those of the mammalian proteins ($+0.260 \pm 0.010$ V) (*1*, *2*) as a result of compensatory effects of less negative reduction enthalpies and entropies. Evaluation of the origin of the difference in $\Delta H^{\circ\prime}_{rc}$ cannot be attempted outside the framework of a suitable theoretical model, given the multiplicity of underlying electrostatic interactions involving the heme, protein charges and dipoles, and solvent dipoles. Likewise, in the absence of solution NMR structures for the plant species, the smaller loss in entropy of these species upon reduction may only be interpreted as indicative of the fact that the two redox states of the plant species differ less in terms of protein flexibility and solvent accessibility of the heme than the mammalian and yeast analogues. It is a fact, however, that the differences in the redox thermodynamics between these two families are not dramatic, indicating that the determinants of the enthalpy and entropy changes are mainly localized in regions of high sequence and structural homology, such as the heme−protein interface.

The biphasic $E^{\circ\prime}/T$ profile observed at or slightly above pH 7 for class I cytochromes was suggested to be the result of a *T*-induced conformational transition between two states of the oxidized form with relatively conserved features at the heme/protein interface, possibly differing in protonation state (*55*, *61*). The close similarity in the temperature of the break point in the above $E^{\circ\prime}/T$ plot (Figure 7a) and in the Curie plots (Figure 9) for the present cytochromes, also observed for mammalian and bacterial species (*25*, *56*), appears to be a conserved feature of class I cytochromes *c*, indicative that the *T*-induced conformational change influ-

ences to some extent the electronic structure of the heme, possibly through a change in orientation of the axial methionine ligand, which is known to strongly affect the distribution of the unpaired spin density across the heme (*14*). The reduction enthalpy and entropy for the high-*T* N_2 conformer are both more negative than those for the low-*T* N_1 species, analogous to that observed for mammalian cyt *c*. Thus, also for the present cytochromes, the decrease in $E^{\circ\prime}$ which characterizes the $N_1 \rightarrow N_2$ transition turns out to be an entirely entropic effect (*25*). The $\Delta\Delta S^{\circ\prime}_{rc}$ and $\Delta\Delta H^{\circ\prime}_{rc}$ values between the N_1 and N_2 conformers invariably increase with increasing pH for all cytochromes *c*, independent of the sources. This effect occurs to a greater extent for the mammalian species as compared to the plant species and the bacterial cyt c_2 (*25*) (Table 1). Although the molecular details of this effect are at present intractable, this clearly indicates that the structural, electronic, and dynamic features of the two redox states of the N_1 and N_2 conformers are influenced by pH in a different way. Likewise, the reason the high-*T* native conformer forms at lower pH values in plant cyt *c* and cyt c_2 as compared to the mammalian species (pH 6.9−7 against 7.5) is at present difficult to explain. It may be due to a more acidic residue which triggers the conformational transition.

The redox behavior of the alkaline conformers (A) of the same species (which are at least two, as indicated by the NMR spectra) is the same, at least within the resolution of the technique. The shape of the voltammetric signal sets the upper value for the difference in reduction potentials, if any, at about 0.015 V. As for other class I cytochromes *c* (*25*), the remarkably lower $E^{\circ\prime}$ of the A form as compared to the N form has mainly an enthalpic origin, related to the much greater stabilization of the ferriheme by the ϵ-amino group of the axially bound lysine which is a much stronger electron donor as compared to the thioether sulfur of the methionine ligand in the neutral form. We note that for the present species the increase in the $\Delta H^{\circ\prime}_{rc}$ values for the A form is such that the reduction becomes a slightly endothermic process (Table 1), at variance with mammalian and bacterial species for which the $\Delta H^{\circ\prime}_{rc}$ values of the A form are still negative (*25*).

Acid−Base Equilibria. Three main pH ranges can be roughly recognized, namely, 2−4, 4−6, and 6−11, in which the pH dependence of the physicochemical parameters of the protein follows distinctive patterns. Below pH 4, the decrease in intensity of the absorption bands at 695 and 530 nm and of the hyperfine-shifted ^{1}H NMR resonances distinctive of the His,Met-ligated low-spin Fe(III) heme and the appearance of the 625 nm absorption band and of a new pattern of ^{1}H NMR resonances typical of high spin-heme Fe(III) are indicative of the disruption of axial heme iron ligation by the protein and its substitution with solvent molecules. This process clearly corresponds to the acidic transition III → II of class I cytochromes *c* which occurs with the same apparent pK_a of 2.5 in other mitochondrial and bacterial species (*1*, *2*). Thus, it is apparent that the thermodynamics of this equilibrium are almost insensitive to changes in the polypeptide matrix surrounding the heme.

In the pH range 5.5−8, the $E^{\circ\prime}$ values, peak currents, and reversibility of the electrochemical process remain constant for all plant cyt *c*. Thus, no acid/base equilibria affect the redox properties of these species in this pH range, as previously observed for the mammalian homologues, and at variance with some bacterial cyt c_2 whose $E^{\circ\prime}$ values were found to be sensitive to the protonation state of a nonliganded histidine residue (*13*, *62*, *63*). This suggests that also in plant cytochromes His26 (conserved in all eukaryotic cyt *c*) and the heme propionate-7 are characterized by low pK_a values. The former residue is known to play an important role in determining the accessibility of the solvent to the hydrophobic core of the cytochrome *c*, influencing the global protein stability and that of the liganding Met80 (*64*). NMR studies on oxidized horse heart cyt *c* revealed that the pK_a of His26 is lower than 3.6, probably due to its nonpolar environment (*2*, *64*, *65*). Such a hydrophobic environment is maintained also in the plant proteins, as clearly shown in the three-dimensional structure of rice cyt *c*, thus suggesting that His26 is characterized by a low pK_a value also in these species. The pK_a of the heme propionate-7 in oxidized mammalian cytochromes *c* is lower than 4.5, while in some bacterial proteins it falls in the range 6−8 (*2*, *63*). We therefore attribute the titration behavior of the Hα peak of the heme propionate-7 of the present proteins with pK_a values of approximately 4.7 (Figure 6a) to an acid−base equilibrium involving this group. These pK_a values are slightly higher than those for the mammalian analogues. The reason for this difference resides in the environment of propionate-7. Although most residues surrounding this group in horse, rice, and spinach cyt *c* are conserved (only Thr40 is substituted by a serine in the plant proteins) and a comparison of the three-dimensional structures of the former two cytochromes shows that also their positions are conserved, a significant difference exists concerning Tyr48. In particular, in rice cyt *c*, the aromatic ring of Tyr48 is parallel to the propionate chain and closer to it as compared to horse cyt *c*, thus making the environment of the propionate chain more hydrophobic in the former protein (*4*). This would stabilize the uncharged form of the propionate, raising its pK_a in plant cytochromes *c* as compared to the mammalian analogues.

The new voltammetric wave II (Figure 1b) and the additional NMR signal pattern which appear above pH 8 (Figure 5) are due to the formation of the low-spin Fe(III) alkaline conformer(s) (state IV) (*26*, *66*). The observation of the anodic counterpart of wave II only for high scan rates indicates that the reduced form of the high-pH species is unstable and transforms rapidly in the corresponding low-pH form, as previously observed for mitochondrial cytochromes *c* and bacterial cytochromes c_2 (*25*, *26*). The different nature of one of the axial ligands, a possible change in the orientation of the imidazole plane of the iron binding histidine, and differences in heme−protein contacts are most likely among the factors responsible for the pH-induced NMR spectral change. The decrease in intensity of the 695 nm absorption band in the electronic spectrum and of the methyl and methylene peaks of the iron-bound methionine in the ^{1}H NMR spectrum shows that also in the present cytochromes the III→IV alkaline transition involves cleavage of the bond between the heme iron and the methionine sulfur. Much experimental evidence indicates lysine residues as the most likely substituting ligands (*29*−*52*, *67*, *68*) whose greater electron donor strength as compared to the native methionine would account for the dramatic decrease in $E^{\circ\prime}$ of the A form as compared to the native conformers, as mentioned above. The existence of two alkaline isomers in

a pH-dependent ratio for all mitochondrial cyt *c* suggested that at least two Lys residues can substitute for the methionine at high pH. Recently, Lys79 and Lys73 were shown to serve as heme ligands in yeast iso-1 cyt *c* (*31*, *32*, *41*), while Lys79 and Lys72 probably play the same role in horse cyt *c* (*31*, *45*, *68*). The residues from positions 70 to 80 are evolutionary conserved in all eukaryotic cytochromes *c*, belonging to the longest highly conserved segment of the polypeptide chain which is proposed to somehow influence the alkaline transition (*68*, *69*). So, it is tempting to propose that Lys79 and -73 are the most probable replacements for the native methionine in axial heme iron ligation at high pH in the plant species. The pK_a values of 8.9 (spinach), 8.4 (cucumber), and 8.4 (sweet potato) obtained from the pH dependence of the current intensity (Figure 3) are in good agreement with the pK_a values of approximately 8.7, 8.4, and 8.3 determined for the same species from the signal intensities in the electronic and NMR spectra (Figures 4b and 6b). It is worthy of note that the *T*-induced decrease in the pK_a for the alkaline transition is more pronounced for the cytochromes *c* from plants as compared to those from mammals. In fact, the resonances of the alkaline form can be observed at pH values as low as 7 upon increasing the temperature above approximately 40 °C (Figure 8). This behavior parallels that of bacterial cyt c_2 (*25*) and indicates that the $\Delta H°$ for the alkaline transition of these species (*33*) must be more positive than that for the same transition in mammalian cyt *c*.

The decrease of the cathodic peak current of wave II at pH higher than 9.5 (not shown) could in principle be due to a protein conformational change leading to an electrochemically silent species *(70)*, but could also be consistent with the coordination of an axial hydroxide ion to the heme iron, whose "hardness" as a nucleophile should induce a remarkably low reduction potential (*32*, *71*).

REFERENCES

1. Scott, R. A., and Mauk, A. G. (1996) *Cytochrome c. A Multidisciplinary Approach*, University Science Books, Sausalito, CA.
2. Moore, G. R., and Pettigrew, G. W. (1990) *Cytochromes c; Evolutionary, Structural and Physicochemical Aspects*, Springer-Verlag, Berlin.
3. Cowan, J. A. (1997) *Inorganic Biochemistry. An Introduction*, Wiley-VCH, New York.
4. Ochi, H., Hata, Y., Tanaka, N., Kakudo, M., Sakurai, T., Aihara, S., and Morita, Y. (1983) *J. Mol. Biol. 166*, 407−418.
5. Kuwana, T. (1977) in *Electrochemical studies of biological systems* (Sawyer, D. T., Ed.) ACS Symposium Series, No. 38, American Chemical Society, Washington, DC.
6. Yee, E. L., Cave, R. J., Guyer, K. L., Tyma, P. D., and Weaver, M. J. (1979) *J. Am. Chem. Soc. 101*, 1131−1137.
7. Yee, E. L., and Weaver, M. J. (1980) *Inorg. Chem. 19*, 1077−1079.
8. Taniguchi, V. T., Sailasuta-Scott, N., Anson, F. C., and Gray, H. B. (1980) *Pure Appl. Chem. 52*, 2275−2281
9. Koller, K. B., and Hawkridge, F. M. (1985) *J. Am. Chem. Soc. 107*, 7412−7417.
10. Inubushi, T., and Becker, E. D. (1983) *J. Magn. Reson. 51*, 128−133.
11. Brown, R., Richardson, M., Scogin, R., and Boulter, D. (1973) *Biochem. J. 131*, 253−256.
12. Unpublished experiments from our laboratory.
13. Battistuzzi, G., Borsari, M., Ferretti, S., Sola, M., and Soliani, E. (1995) *Eur. J. Biochem. 232*, 206−213.
14. Bertini, I., Turano, P., and Vila, A. J. (1993) *Chem. Rev. 93*, 2833−2932.
15. Banci, L., Bertini, I., Bren, K. L., Gray, H. B., Sompornpisut, P., and Turano, P. (1997) *Biochemistry 36*, 8992−9001.
16. Banci, L., Bertini, I., Gray, H. B., Luchinat, C., Redding, T., Rosato, A., and Turano, P. (1997) *Biochemistry 36*, 9867−9877.
17. Gao, Y., Boyd, J., Williams, R. J. P., and Pielak, G. J. (1990) *Biochemistry 29*, 6994−7003.
18. Feng, Y. G., Roder, H., Englander, S. W., Wand, A. J., and Di Stefano, D. L. (1989) *Biochemistry 28*, 195−203.
19. Smith, G. M., and Yu, L. P. (1991) *Biochim. Biophys. Acta 1058*, 75−78.
20. Yu, L. P., and Smith, G. M. (1990) *Biochemistry 29*, 2914−2919.
21. Yu, L. P., and Smith, G. M. (1990) *Biochemistry 29*, 2920−2925.
22. Taniguchi, I., Funatsu, T., Iseki, M., Yamaguchi, H., and Yasukouchi, K. (1985) *J. Electroanal. Chem. 193*, 295−302.
23. Eddowes, M. J., and Hill, H. A. O. (1977) *J. Chem. Soc., Chem. Commun.*, 771−772.
24. Bond, A. M., and Hill, H. A. O. (1991) *Met. Ions Biol. Syst. 27*, 431−494.
25. Battistuzzi, G., Borsari, M., Sola, M., and Francia, F. (1997) *Biochemistry 36*, 16247−16258.
26. Barker, P. D., and Mauk, A. G. (1992) *J. Am. Chem. Soc. 114*, 3619−3624.
27. Pettigrew, G. W., Bartsch, R. G., Meyer, T. E., and Kamen, M. D. (1978) *Biochim. Biophys. Acta 503*, 509−523.
28. Pettigrew, G. W., Meyer, T. E., Bartsch, R. G., and Kamen, M. D. (1975) *Biochim. Biophys. Acta 430*, 197−208.
29. Banci, L., Bertini, I., Spyroulias, G. A., and Turano, P. (1998) *Eur. J. Inorg. Chem.* 583−591.
30. Wilson, M. T., and Greenwood, C. (1996) in *Cytochrome c. A Multidisciplinary Approach* (Scott, R. A., and Mauk, A. G., Eds.) pp 611−634, University Science Books, Sausalito, CA.
31. Rosell, F. I., Ferrer, J. C., and Mauk, A. G. (1998) *J. Am. Chem. Soc. 120*, 11234−11245.
32. Döpner, S., Hildebrandt, P., Rosell, F. I., and Mauk, A. G. (1998) *J. Am. Chem. Soc. 120*, 11234−11245.
33. Taler, G., Schejter, A., Navon, G., Vig, I., and Margoliash, E. (1995) *Biochemistry 34*, 14209−14212.
34. Colon, W., Wakem, L. P., Sherman, F., and Roder, H. (1997) *Biochemistry 36*, 12535−12541.
35. Pollock, W. B. R., Rosell, F. I., Twitchett, M. B., Dumont, M. E., and Mauk, A. G. (1998) *Biochemistry 37*, 6124−6131.
36. Dixon, D. W., Hong, X., and Woehler, S. E. (1989) *Biophys. J. 56*, 339−351.
37. Jordan, T., Eads, J. C., and Spiro, T. G. (1995) *Protein Sci. 4*, 716−728.
38. Schejter, A., and George P. (1965) *Biochemistry 3*, 1045−1049.
39. Babul, J., and Stellwagen, E. (1972) *Biochemistry 11*, 1195−1200.
40. Hong, X., and Dixon, D. W. (1989) *FEBS Lett. 246*, 105−108.
41. Ferrer, J. C., Guillemette, J. G., Bogumil, R., Inglis, S. C., Smith, M., and Mauk, A. G. (1993) *J. Am. Chem. Soc. 115*, 7507−7508.
42. Pearce, L. L., Gärtner, A. L., Smith, M., and Mauk, A. G. (1989) *Biochemistry 28*, 3152−3156.
43. Angstrom, J., Moore, G. M., and Williams, R. J. P. (1982) *Biochim. Biophys. Acta 703*, 87−94.
44. Davis, L. A., Schejter, A., and Hess, G. P. (1974) *J. Biol. Chem. 249*, 2624−2632.
45. Smith, H. T., and Millett, F. (1980) *Biochemistry 19*, 1117−1120.
46. Lambeth, D. O., Campbell, K. L., Zand, R., and Palmer, G. (1973) *J. Biol. Chem. 248*, 8130−8136.
47. Osheroff, N., Borden, D., Koppenol, W. H., and Margoliash, E. (1980) *J. Biol. Chem. 255*, 1689−1697.
48. Wooten, J. B., Cohen, J. S., Vig, I., and Schejter, A. (1981) *Biochemistry 20*, 5394−5402.

49. Gadsby, P. M. A., Peterson, J., Foote, N., Greenwood, C., and Thomson, A. J. (1987) *Biochem. J. 246*, 43−54.
50. Nall, B. T., Zuniga, E. H., White, T. B., Wood, L. C., and Ramdas, L. (1989) *Biochemistry 28*, 9834−9839.
51. Schejter, A., Luntz, T. L., Koshy, T. I., and Margoliash, E. (1992) *Biochemistry 31*, 8336−8343.
52. Ubbink, M., Warmerdam, G. C. M., Campos, A. P., Teixeira, M., and Canters, G. W. (1994) *FEBS Lett. 351*, 100−104.
53. Taniguchi, I., Iseki, M., Takaki, E., Toyosawa, K., Yamaguchi, H., and Yasukouchi, K. (1984) *Bioelectrochem. Bioenerg. 13*, 373−383.
54. Koller, K. B., and Hawkridge, F. M. (1988) *J. Electroanal. Chem. 239*, 291−306.
55. Ikeshoji, T., Taniguchi, I., and Hawkridge, F. M. (1989) *J. Electroanal. Chem. 270*, 297−308.
56. Benini, S., Borsari, M., Ciurli, S., Dikiy, A., and Lamborghini, M. (1998) *JBIC, J. Biol. Inorg. Chem. 3*, 371−382.
57. Bertrand, P., Mbarki, O., Asso, M., Blanchard, L., Guerlesquin, F., and Tegoni, M. (1995) *Biochemistry 34*, 11071−11079.
58. Frolov, E. N., Gvosdev, R., Goldanskii, V. I., and Parak, F. G. (1997) *JBIC, J. Biol. Inorg. Chem. 2*, 710−713.
59. Banci, L., Gori-Savellini, G., and Turano, P. (1997) *NATO ASI Ser., Ser. 3, 41* (Molecular Modeling and Dynamics of Bioinorganic Systems), 191−216.
60. Cohen, D. S., and Pielak, G. J. (1995) *J. Am. Chem. Soc. 117*, 1675−1677.
61. Christen, R. P., Nomikos, S. I., and Smith, E. T. (1996) *JBIC, J. Biol. Inorg. Chem. 1*, 515−522.
62. Pettigrew, G. W., Bartsch, R. G., Meyer, T. E., and Kamen, M. D. (1978) *Biochim. Biophys. Acta 503*, 509−523.
63. Moore, G. R., Harris, D. F., Leitch, F. A., and Pettigrew, G. W. (1984) *Biochim. Biophys. Acta 764*, 331−342.
64. Qin, W., Sanishvili, R., Plotkin, B., Schejter, A., and Margoliash, E. (1995) *Biochim. Biophys. Acta 1252*, 87−94.
65. Cohen, J. S., Fischer, W. R., and Schechter, A. N. (1974) *J. Biol. Chem. 249*, 5472−5437.
66. Haladjian, J., Pilard, R., Bianco, P., and Serre, P.-A. (1982) *Bioelectrochem. Bioenerg. 9*, 91−101.
67. Gadsby, P. M. A., Peterson, J., Foote, N., Greenwood, C., and Thomson, A. J. (1987) *Biochem. J. 246*, 43−54.
68. Theodorakis, J. L., Garber, E. A. E., McCracken, J., Peisach, J., Schejter, A., and Margoliash, E. (1995) *Biochim. Biophys. Acta 1252*, 103−113.
69. Davis, L. A., Schejter, A., and Hess, G. P. (1974) *J. Biol. Chem. 249*, 2624−2632.
70. Eddowes, M. J., and Hill, H. A. O. (1979) *J. Am. Chem. Soc. 101*, 4461−4464.
71. Li, Y., Imaeda, K., and Inokuchi H. (1994) *J. Phys. Chem. 98*, 4726−4728.

BI982429X